

Self-spreading high-temperature synthesis of TiB_2 powder

B. SHAHBAHRAMI^{1*}, R. SARRAF MAAMOORI², N. EHSANI¹

¹Faculty of Materials Science and Engineering, Malek-e-Ashtar University, P.O. Box 15875, Tehran, I.R. Iran

²Faculty of Engineering, Tarbiat Modares University, P.O. Box 14115-111, Tehran, I.R. Iran

$\text{TiB}_2/\text{Al}_2\text{O}_3$ powder composite was synthesized via simultaneous aluminum reduction of TiO_2 and B_2O_3 according to self-spreading high temperature (SHS) reaction in an oxidizing atmosphere. Using controlled atmosphere and high temperature is not necessary in this method. Based on the Taguchi experimental technique, various experiments were carried out and some characteristic parameters were determined. Due to the formation of intermolecular phases between Al_2O_3 and CaO which are soluble in HCl , CaO powder was added to the starting materials to make pure TiB_2 . The most appropriate powder was obtained from the materials of stoichiometric composition, purified with an optimum amount of HCl . Characteristics of the produced samples were studied with X-ray diffraction, atomic absorption spectroscopy and particle size analysis.

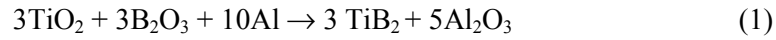
Key words: *titanium diboride; SHS; aluminothermic reaction; Taguchi experimental design*

1. Introduction

TiB_2 with a high melting point and high hardness [1, 2], relatively low density [3], good electrical and thermal conductivity [4], and chemical resistance [5, 6] is a suitable candidate for applications such as refractory materials, nozzles, light armours, coatings, etc. [7–11]. In this work, the method of self-spreading high temperature synthesis (SHS), which is simple, low-cost, and needs no expensive facilities, was used. It also enables one to produce TiB_2 powder at low temperatures and in very short time [10, 12]. In the SHS method, the material is produced by thermal energy generated during the chemical reaction between precursor materials. The process begins with external heating, and then sufficient heat is generated by the chemical reaction between raw materials [13]. The powder produced has a very fine particle size, high surface area, and high reactivity. The powder can be sintered at 1300–1500 °C, while

* Corresponding author, e-mail: behmut@yahoo.com

the powders produced by other techniques sinter at 1800–2200 °C [10, 12]. In this method, besides TiB₂, Al₂O₃ powder is also obtained as a product. Since Al₂O₃ is a material with a high melting point and high chemical resistance, its separation by chemical methods is difficult [14]. The addition of CaO to the precursor materials leads to the formation of an intermolecular phase (CaO–Al₂O₃–B₂O₃) which is soluble in HCl [14, 15]. The reaction between TiO₂, B₂O₃, and Al powders is as follows:



The effects of various parameters such as time, temperature, particle size of Al, B₂O₃, and TiO₂ powders, and the amount of Al and B₂O₃ powders on the produced TiB₂ were studied in this work.

2. Experimental procedures

The characteristics of the materials used are shown in Table 1. In this experiment, raw materials were mixed by a vibrator (200, Octagon). Then the batches (15 g) of mixed powders were heated in an electric furnace at various temperatures and times. The final products were milled using a planetary mill (6 Pulverisette, Fritsch), to make fine powders.

Table 1. The materials used

Raw material	Particle size [μm]	Purity [%]
Fine Al powder (F)	F < 44	99
Coarse Al powder (C)	63 < C < 149	99
Fine TiO ₂ powder (F)	F < 44	99.9
Coarse TiO ₂ powder (C)	63 < C < 149	99.9
Fine B ₂ O ₃ powder (F)	F < 44	99.9
Coarse B ₂ O ₃ powder (C)	63 < C < 149	99.9
Coarse CaO powder (C)	63 < C < 149	99.9

Using the Taguchi method, four levels and four parameters were selected (Table 2). In fact, before arranging the final process, eight experimental trials have been carried out and the effects of TiO₂, B₂O₃, and Al particle sizes were studied. The final experiments were arranged basing on the calculated coefficient k and the particle size groups were selected;

$$k = \frac{I_{100\text{TiB}_2}}{\sum I_{100}} \times 100\%$$

where $I_{100\text{TiB}_2}$ is the intensity of the peak due to TiB₂, and I_{100} is a sum of peak intensities due to all phases existing in the sample.

In accordance with previous papers, four parameters (time, temperature, and the amounts of Al and B_2O_3 powders) were selected [16]. Therefore, with 5 factors and 4 variable levels, 16 experiments were performed according to the Taguchi experimental design (Table 3). The best processing conditions have been identified from the experimental results (k). This experiment was repeated with CaO powder addition to the precursor powders (TiO_2 , B_2O_3 and Al). The effect of CaO amount on the process was studied with the addition of various amounts of CaO powder (stoichiometric amount, 20 wt. % and 30 wt. % more than stoichiometric amount).

2. Variable levels and parameters

Parameter	Level			
	1	2	3	4
a) Particle size ¹⁾	F. F.F	F.F.C.	F.C.C	C.C.F
Temperature [°C]	950	1050	1250	1350
Time [h]	0.5	1	1.5	2
b) Al powder content ²⁾	1	1.1	1.2	1.3
b) B_2O_3 powder content	1	1.1	1.2	1.3

¹a) – the letters represent particle size of TiO_2 , B_2O_3 and Al powders, respectively, from left to right.

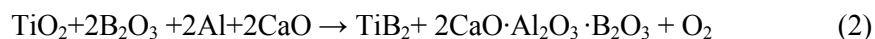
²b) – Al and B_2O_3 powder contents are given based on the stoichiometric amounts (Eq. (1)).

Table 3. Experimental design

No.	Particle size	Temperature [°C]	Time [h]	Al powder content (stoichiometric ratio)	B_2O_3 powder content (stoichiometric ratio)	$K^{(1)}$
n_1	F.F.F	950	0.5	1	1	12.67
n_2	F.F.F	1050	1	1.1	1.1	23.78
n_3	F.F.F	1250	1.5	1.2	1.2	46.94
n_4	F.F.F	1350	2	1.3	1.3	2.99
n_5	F.F.C	950	1	1.2	1.3	22.05
n_6	F.F.C	1050	0.5	1.3	1.2	26.28
n_7	F.F.C	1250	2	1	1.1	7.69
n_8	F.F.C	1350	1.5	1.1	1	12.45
n_9	F.C.C	950	1.5	1.3	1.1	0
n_{10}	F.C.C	1050	2	1.2	1	2.15
n_{11}	F.C.C	1250	0.5	1.1	1.3	7.71
n_{12}	F.C.C	1350	1	1	1.2	0
n_{13}	C.C.F	950	2	1.1	1.2	18.22
n_{14}	C.C.F	1050	1.5	1	1.3	8.48
n_{15}	C.C.F	1250	1	1.3	1	37.67
n_{16}	C.C.F	1350	0.5	1.2	1.1	43.62

⁽¹⁾ K is the average of repeated experiments

The reaction between stoichiometric amounts of precursor materials was as follows [14, 15]:



The best sample (which had the highest amount of TiB_2) was treated with HCl to wash the impurities. Three different concentrations of HCl (pH equal to 1, 2 and 3) were used and each sample was passed through paper. After washing it a few times with deionized water, it was dried for 2 h. The phases formed in the samples were determined by the XRD (PW 1830, Philips). The particle size of the specimens was measured using a laser particle size analyzer (A22, Fritsch). The chemical composition was characterized by the atomic absorption spectroscopy (Pye Unicam SP9, Philips).

3. Results and discussion

Table 4 shows the effect percentage of variable parameters on the amount of the TiB_2 phase formed (K). These data were calculated using the Taguchi method. As is shown in the table, the coefficient of variation (CV) is relatively high. The most probable reason for this is the heat generated in the SHS reaction. Therefore, the measurement of temperature may not be accurate.

Table 4. The effect of parameters on the K index

Parameter		$K_{\text{ave.}}$	Variance (S^2)	Standard deviation (S)	Coefficient of variation (CV) [%]	Effect percentage on K
Temperature	Level 1	13.23	39.72	6.30	48	9.97
	Level 2	15.17	58.83	7.67	51	
	Level 3	25	177.21	13.31	53	
	Level 4	14.76	170.66	13.06	88	
Time	Level 1	22.57	110.8	10.53	47	15.14
	Level 2	20.87	103.95	10.20	49	
	Level 3	16.97	182.67	13.52	80	
	Level 4	7.76	23.38	4.84	62	
Al amount	Level 1	7.20	11.95	3.46	48	27.05
	Level 2	15.50	20.85	4.57	29	
	Level 3	28.70	186.35	13.65	48	
	Level 4	16.70	142.62	11.94	71	
B_2O_3 amount	Level 1	16.20	97.84	9.89	61	9.54
	Level 2	18.80	159.67	12.64	67	
	Level 3	22.90	162.24	12.74	56	
	Level 4	10.30	28.79	5.37	52	
Particle size	Level 1	21.59	153.28	12.38	57	38.30
	Level 2	17.17	31.28	5.59	33	
	Level 3	2.46	5.68	2.38	97	
	Level 4	27	115.74	10.76	40	

Figure 1 shows the effect of temperature on the formation of the TiB_2 phase (K_{ave} – average dependent variable). In this system, the boron oxide melts at 450 °C [11] and evaporates above 450 °C. Therefore, due to the B_2O_3 evaporation from the system at temperatures higher than 450 °C, its amount decreases upon increasing temperature [10, 16]. TiO_2 is solid in the reaction conditions. However, Al powder melts at 660 °C and reduces B_2O_3 and TiO_2 . Then, boron (B) reacts with titanium (Ti) through the liquid–solid mechanism. At temperatures higher than 1000 °C, the gas–solid mechanism is predominant, and as a result the rate of the reaction increases [11, 16, 17].

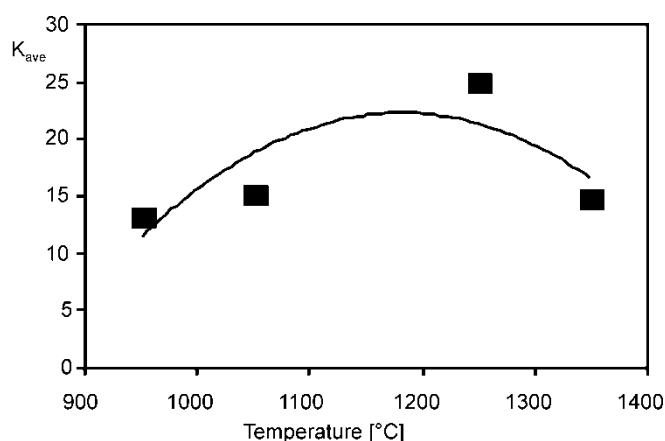


Fig. 1. Effect of temperature on TiB_2 phase formation

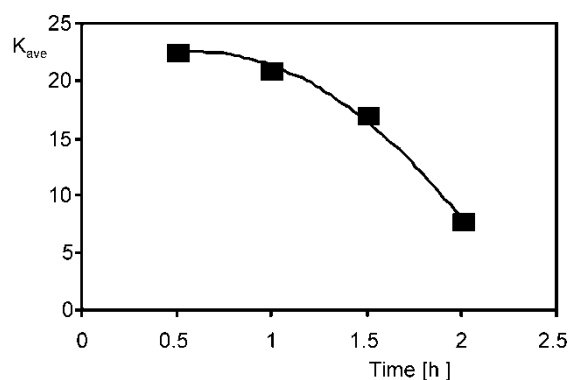


Fig. 2. Effect of time on TiB_2 phase formation

When the temperature increases, more B_2O_3 evaporates from the system. Therefore, sufficient amount of boron is not available to react with the entire titanium, thus the amount of TiB_2 decreases. It can be concluded that above 1170 °C, temperature has a negative effect on TiB_2 formation. As can be seen in Table 4, compared to the other variables, the effect of temperature is not remarkable because the rate of B_2O_3

evaporation rises with the increase of temperature. Furthermore, in the SHS or thermite reactions, when temperature enhances to a specific level, they proceed independently. Therefore, heating is only needed for the initiation of the reaction [18].

The effect of time on the TiB_2 formation is shown in Figure 2. This figure shows that the amount of TiB_2 formed decreases with time. With time, more B_2O_3 evaporates from the system. Thermite or SHS reactions are very fast, being accomplished in a very short time. In these reactions, temperature increases rapidly. Even under such conditions, the reaction needs some time to be completed [16, 19]. Therefore, 30 min was the minimum time applied.

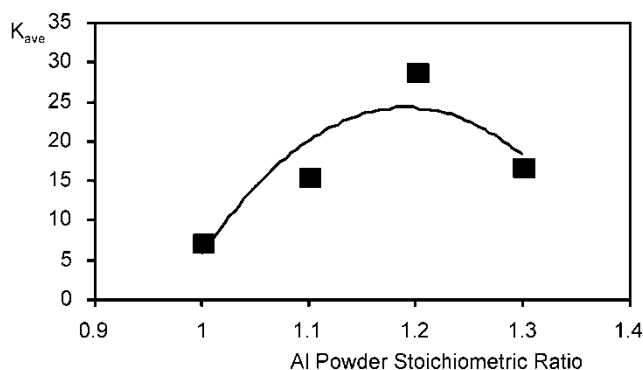


Fig. 3. Effect of Al powder content on TiB_2 phase formation

The effect of the amount of Al powder on the TiB_2 formation is presented in Fig. 3. By increasing the amount of Al powder (above the stoichiometric amount), the formation of TiB_2 also accelerated. This is due to the reduction mechanism of boron oxide and titanium oxide by the Al powder. In this mechanism, when the amount of Al powder increases, more B_2O_3 and TiO_2 were reduced by the Al powder. In addition, increasing the Al powder amount can hinder the escape of B_2O_3 [10, 16]. However, if the amount of Al powder increases by more than a certain value, it can cause an inverse effect on the amount of TiB_2 produced. In such a case, impurities such as Al, Al_2O_3 , and compositions of Al and B are developed in the system. Compared to other parameters, the effect of this parameter on the TiB_2 formation (27.05%) was the most efficient. The optimum level of aluminum is 1.19.

Figure 4 shows the effect of B_2O_3 amount on the TiB_2 formation. The vapour pressure of boron oxide is high, thus high temperature leads to a rapid evaporation of B_2O_3 . As a result, the level of boron oxide (B_2O_3) in the starting composition should be larger than its stoichiometric level [10, 16, 20–22]. Insufficient amount of boron oxide leads to the formation of an inadequate amount of TiB_2 . In this case, the unreacted TiO_2 and Al are present in the final product. The amount of TiB_2 formed was raised by increasing the quantity of B_2O_3 up to an optimum level. Above this level, the additional Al reacted with B. Therefore, a sufficient amount of B was not available in the system to react with Ti. As a result, the impurities such as TiO_2 and various com-

positions of Al and Ti formed and the amount of TiB_2 decreased. So, the best level of B_2O_3 ratio was 1.12.

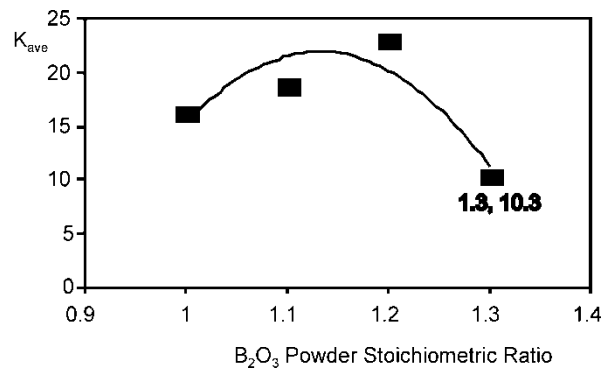


Fig. 4. Effect of B_2O_3 powder amount on TiB_2 formation

The effect of particle size on the yield of TiB_2 powder is illustrated in Fig. 5. As can be seen in this figure, group 4 of the starting materials gave the best result. It was found that decreasing the Al powder particle size increases the amount of TiB_2 produced. Therefore, batches containing powders with particle size characteristic of C.C.F. (coarse B_2O_3 and TiO_2 powders with fine Al powder) had the highest production yield.

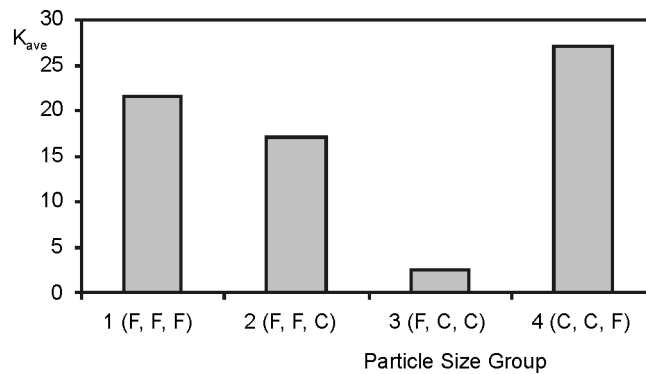


Fig. 5. Effect of particle size on TiB_2 formation

The effect of the CaO additive (according to the stoichiometric ratio, 20 wt. % and 30 wt. % over the stoichiometric ratio) on the XRD patterns of the final product is shown in Fig. 6. The patterns show that TiB_2 , Al_2O_3 , and CaAlB_3O_7 phases are present in each of them. It seems that the amount of amorphous phases increased with increasing amount of CaO powder. Therefore, due to the addition of CaO powder, the possibility of phase crystallization decreased. Furthermore, the SHS method is very fast, thus there is not enough time for crystallization in this technique [15].

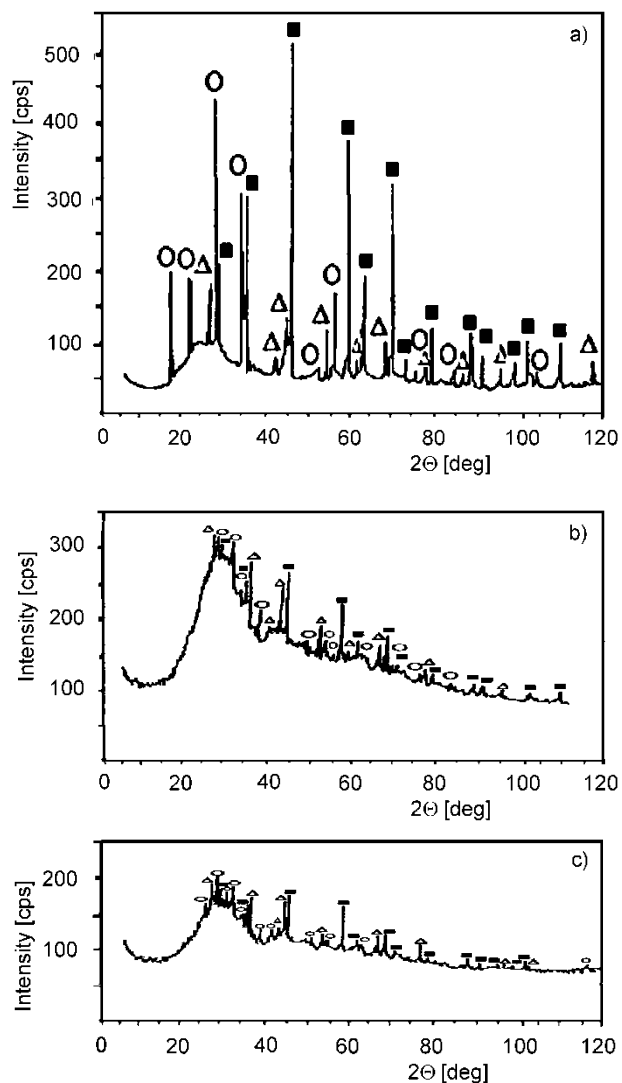


Fig. 6. XRD patterns of synthesized samples using CaO powder in: a) stoichiometric ratio, b) 20 wt. % above the stoichiometric ratio, and c) 30 wt. % above the stoichiometric ratio; \circ – CaAlB_3O_7 , Δ – Al_2O_3 , \blacksquare – TiB_2

The k index of the specimens was 53 wt. %, 50 wt. %, and 45 wt. % for the synthesized powder using CaO powder in the stoichiometric ratio, and 20 wt. % and 30 wt. %, respectively.

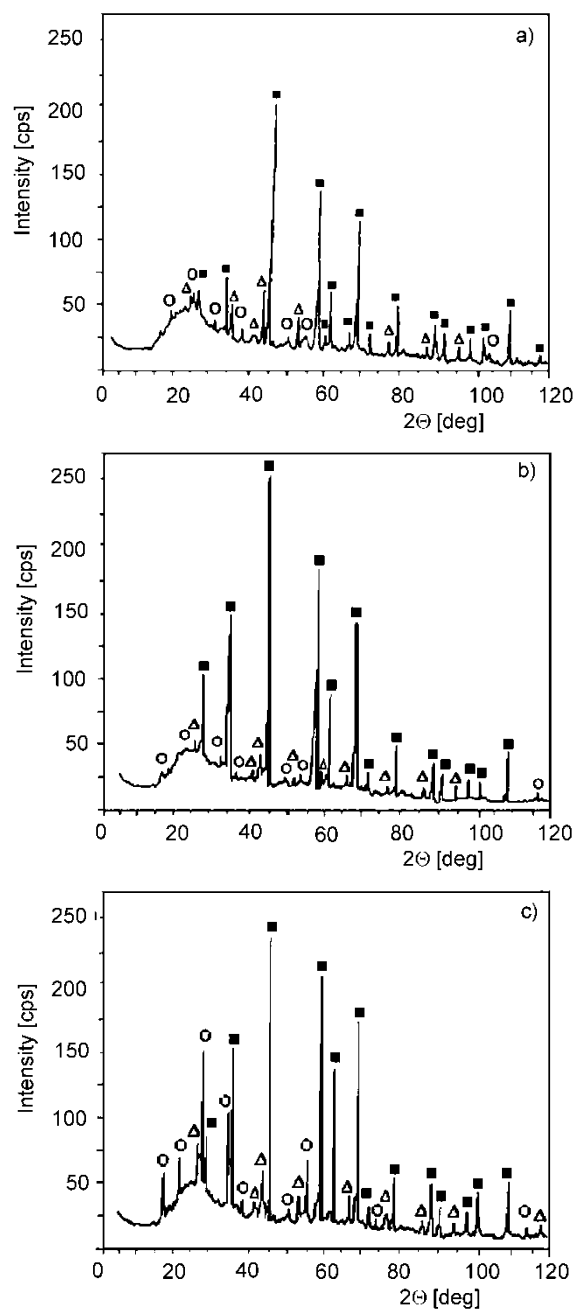


Figure 7. XRD pattern of purified sample (powder):
a) pH = 1, b) pH = 2, c) pH = 4; \circ – CaAlB_3O_7 , Δ – Al_2O_3 , \blacksquare – TiB_2

Then, the samples obtained from stoichiometric amounts of precursor materials were treated with HCl. XRD patterns of purified specimens at various pH are presented in Fig. 7. The patterns show that after purification three phases (TiB_2 , Al_2O_3 and CaAlB_3O_7) still exist in the specimens. It can be concluded that a perfect purification is not possible by this method. However, the intensity of CaAlB_3O_7 peaks decrease in the purified samples. Simultaneously, the intensities of TiB_2 peaks increase in the treated specimens. This was also confirmed by atomic absorption spectroscopy (AAS). Table 5 shows the atomic absorption spectroscopy results for the purified and unpurified powders. It can be seen that Ti content increases with purification and its maximum level was measured in the purified samples at pH = 2. It also shows that Ca and Al contents decrease with purification and their minimum level was obtained in the purified samples at pH = 2.

Table 5. AAS of the purified and unpurified powders

Sample	Ti [wt. %]	B [wt. %]	Al [wt. %]	Ca [wt. %]
Unpurified	34	25	16	14
Purified (pH = 1)	52	25	19	2
Purified (pH = 2)	60	28	10	0.65
Purified (pH = 4)	41	27	17	11

The measured K indices of the treated and untreated specimens are presented in Table 6. The table shows that the K index and TiB_2 wt. % increase with treatment. The highest K index (TiB_2) was obtained for the purified sample at pH = 2. On the other hand, the amount of the CaAlB_3O_7 phase decreases with purification and reaches its minimum level when purified at pH = 2. It is evident that at a low concentration of HCl (pH = 4), the lowest amount of CaAlB_3O_7 impurity was eliminated. However, at a high concentration of HCl (pH = 1), in addition to the elimination of CaAlB_3O_7 , a considerable amount of TiB_2 was also washed away with HCl. Therefore, due to the decreasing CaAlB_3O_7 and TiB_2 content, the content of Al_2O_3 increases. It can be concluded that because of a high chemical resistance of Al_2O_3 against acids and alkalis, it cannot be washed out in HCl [23, 24]. The best result was obtained with a moderate concentration of HCl (pH = 2). Under such conditions, without the elimination of TiB_2 , a significant amount of CaAlB_3O_7 was removed.

Table 6. The K index and amounts of the phases

Sample	K	TiB_2 [wt. %]	Al_2O_3 [wt. %]	CaAlB_3O_7 [wt. %]
Unpurified	53	58	7	35
Purified (pH = 1)	80	75.5	18	5
Purified (pH = 2)	91	87	10	2
Purified (pH = 4)	63	60	10	27

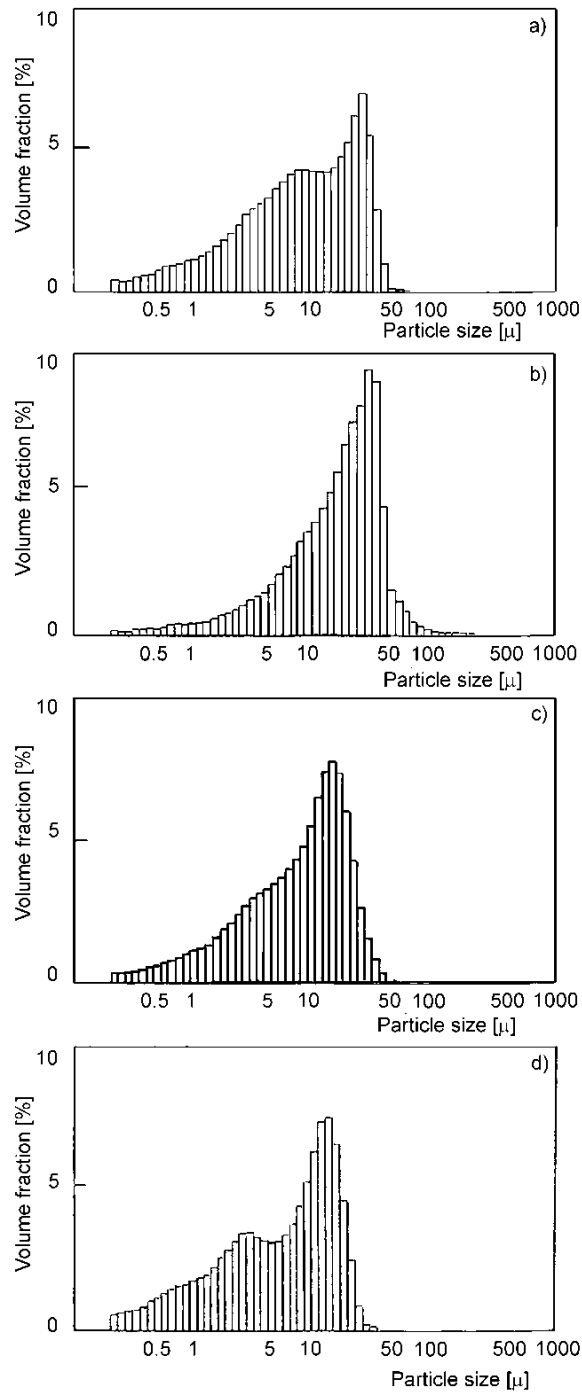


Fig. 8. Particle size distribution of: a) purified sample at pH = 4, b) purified sample at pH = 2, c) purified sample at pH = 1, d) unpurified sample

Figure 8 shows the particle size distribution of the purified and unpurified samples. In these figures, the vertical axis indicates volume fractions percent of particle sizes, the sum of which is 100 percent. A comparison between the figures demonstrates that the unpurified samples (with $d_{50} < 7.41\mu\text{m}$) have the finest particle size. The purified sample at $\text{pH} = 2$ (with $d_{50} < 21.76\mu\text{m}$) has the most coarse particle size. A comparison between these data and Table 6 reveals that the purification increases the particle size. Therefore, it can be assumed that the impurities are smaller than TiB_2 particles.

4. Conclusions

The optimum temperature for TiB_2 powder formation was 1170°C . Compared to other methods, this is a low temperature. Beyond 30 min, the amount of TiB_2 formed decreases upon increasing time. Increasing the B_2O_3 and Al amounts above their stoichiometric values had a significant effect on TiB_2 powder formation. Particle size of the precursor powder had a pronounced effect on TiB_2 powder formation. Fine Al powder plus coarse B_2O_3 and TiO_2 powders led to the highest amount of products. Addition of CaO powder led to the reduction of Al_2O_3 and formation of CaAlB_3O_7 , which is soluble in HCl. It decreased phase crystallization and caused amorphous powder formation. The optimum amount of CaO additive was equal to its stoichiometric level. The most suitable purification conditions were those with $\text{pH} = 2$, although a perfect elimination of impurities is not possible. A more efficient purification led to the production of a coarser powder.

References

- [1] KANG E.S., JANG C.W., J. Am. Ceram. Soc., 72 (1989), 1868.
- [2] RICCI R., MATTEAZZI R., Mater. Sci. Eng. A, 379 (2004), 341.
- [3] SHI L., GU Y., CHEN L., YANG Z., MA J., QIAN Y., Inorg. Chem. Commun., 7 (2004), 192.
- [4] SCHNEIDER J., *Engineering Materials Handbook*, ASM International, 1991.
- [5] WEIMER A.W., *Carbide, Nitride and Boride Materials Synthesis and Processing*, Chapman & Hall, London, 1997.
- [6] MANDORF V., HARTWIG J., SELDIN E.J., *High Temperature Deformation of Titanium Diboride*, [in:] G.M. Ault (Ed.), *High Temperature Materials*, Vol. 2, Wiley-Interscience, New York, 1963, p. 455.
- [7] BAIK S., BECHER P.F., J. Am. Ceram. Soc., 70 (1987), 527.
- [8] CAPUTO A.J., LACKEY W.J., J. Electrochem. Soc., 132 (1985), 2274.
- [9] BAUMGARTNER H.R., STEIGER R.A., J. Am. Ceram. Soc., 67 (1984), 207.
- [10] LOGAN K.V., U.S. Patent 5 160 716, 1992.
- [11] CHEN L., GU Y., QIAN Y., SHI L., YANG Z., MA J., Mater. Res. Bull., 39 (2004), 609.
- [12] LOGAN K.V., U.S. Patent 4 888 166, 1989.
- [13] MOSSINO P., DEORSOLA F.A., VALLAURI D., AMATO I., Ceram. Int., 30 (2004), 2229.
- [14] ANDRIEUX J.L., PEFFEN R., U.S. Patent 3 016 288, 1962.
- [15] YI ET AL., U.S. Patent, 6 645 424, 2003.
- [16] LOGAN K.V., WALTON J.D., Ceram. Eng. Sci. Proc., 5 (1984), 712.

- [17] WALTON J.D., POULOS N.E., J. Am. Ceram. Soc., 42 (1959), 40.
- [18] MERIC C., ENGEZ T., Welding J., Jan. (1999), 33.
- [19] GEIGER M.J., POIRIER D., Welding J., 61 (1999), 260.
- [20] WALKER J.K., Adv. Ceram. Mater., 3 (1988), 601.
- [21] WEIMER A.W., MOORE W.G., ROACH R.P., HITT J.E., DIXIT R.S., J. Am. Ceram. Soc., 75 (1992), 2509.
- [22] TIMMS P.L., U. S. Patent 3 351 429, 1967.
- [23] LEE W.E., *Ceramic Microstructure*, Chapman & Hall, New York, 1994.
- [24] GITZEN W., *Alumina as a Ceramic Material*, The American Ceramic Society, Columbus, OH, 1970.

Received 6 January 2007

Revised 6 February 2007